

Corrosion Inhibition Potential of Ethanol Extract of *Bryophyllum pinnatum* Leaves for Zinc in Acidic Medium

Alhaji Modu Kolo^{1*}, Sunusi Idris², Oloyede Martins Bamishaiye³

¹Department of Chemistry, Corrosion Protection and Material Science Laboratory, Abubakar Tafawa Balewa University, Bauchi, Nigeria; nocaseoche@yahoo.com (A.M.K).

²Department of Chemistry, Kano University of Science and Technology, Wudil, Nigeria

³Department of General Studies, Federal College of Agricultural Produce Technology Kano, Nigeria

Abstract: The inhibitive and adsorption properties of ethanol extract of *Bryophyllum pinnatum* leaves were studied using weight loss, potentiodynamic polarization, Scanning Electron Microscopy (SEM) and Fourier transformed infra-red spectroscopy (FTIR) methods of monitoring corrosion. The results obtained, indicated that ethanol extracts of *Bryophyllum pinnatum* leaves is a good adsorption inhibitor for the corrosion of zinc in sulphuric acid solutions. The adsorption of the inhibitor on zinc surface was found to be spontaneous and supported the Langmuir adsorption model. From the calculated values of free energy of adsorption, the activation energy and the variation of inhibition efficiency with temperature, a physical adsorption mechanism has been proposed for the adsorption of ethanol extract of *Bryophyllum pinnatum* leaves on zinc surface. Results from potentiodynamic polarization study indicated that *Bryophyllum pinnatum* is a mixed-type corrosion inhibitor. Analysis of spectra obtained from Fourier transformed infra-red spectrophotometer (FTIR) revealed that some functional groups presence in the spectra of the inhibitors were missing in the spectra of the corrosion products which also indicated that there is an interaction between zinc and the inhibitor.

Keywords: Adsorption; Corrosion; Green inhibitor; *Bryophyllum pinnatum* leaves.

1. Introduction

The consequences of corrosion are enormous in the metallurgical industries where metal components or their alloys are used in the fabrication of different materials or components for engineering and other industrial use. Zinc metal for instance is applied in many areas some of which includes reaction vessels, pipes, tanks, etcetera which are known to corrode invariably in contact with various solvents. The study of corrosion of zinc is a matter of tremendous theoretical and practical concern, and as such has received a considerable amount of interest. Acid solutions widely used in industrial acid cleaning, acid de-scaling, acid pickling and oil well acidizing, require the use of corrosion inhibitors in order to restrain their corrosion attack on metallic materials. Inhibitors are chemicals that react with the surface of a material decreasing the material's corrosion rate, or interact with the operating environment to reduce its corrosivity [1]. Most of the corrosion inhibitors available are synthetic chemicals, expensive and very hazardous to the environment. Therefore, it is desirable to source for environmentally safe, economical, green inhibitors [2-4]. There has been a wide spread research on the use of plant extracts and their isolates as corrosion inhibitors. Hence, a vast number of natural plants are continuously been investigated as profitable alternatives to synthetic inhibitors because of their obvious advantages which include among other things, their ready availability, biodegradability, non-toxicity, non-pollutancy and eco-friendliness [1, 5-7]. Leave extracts of *Bryophyllum pinnatum* are tested for the first time as corrosion inhibitors in this work. Hence, this research work is aimed at investigating the inhibitive and adsorptive properties of ethanol extract of *Bryophyllum pinnatum* leaves for the corrosion of zinc in 0.1M H₂SO₄ which will be achieved through the following objectives

- (i) Evaluation of corrosion of zinc in H₂SO₄ by gravimetric-based mass loss.
- (ii) Phytochemical composition of ethanol extract of *Bryophyllum pinnatum* leaves in the chemical laboratory using various standard phytochemical screening methods.
- (iii) Undertake potentiodynamic polarization studies of the inhibition of zinc by the *Bryophyllum pinnatum* leaves extract.
- (iv) Using Fourier Transform Infrared (FTIR) spectroscopy to investigate the functional groups in the plant extract and the corrosion product.
- (v) Characterization of the test coupons before and after the corrosion tests using Scanning Electron Microscopy (SEM).
- (vi) Proposition of model/mechanism of inhibition by the ethanol extract of *Bryophyllum pinnatum* leaves from generated parameters

2. Materials and Methods

2.1. Materials

The sheets of zinc, A72357 type used for this study were obtained from the Novara group Limited England. The composition of the zinc metal in (% wt) as determined by quantitative method of analysis, using X-ray fluorescence spectrometer of PANALYTICAL model MagiX is Zn (99.548), Pb (0.004), Al (0.001), Cu (0.347), Cd (0.013), Sn (0.001), Fe (0.001) and Ni (0.085). Each sheet was 0.4 mm in thickness and were mechanically pressed cut into 5 x 4 cm coupons. The coupons were degreased by washing in absolute ethanol, dried in acetone and stored in moisture free desiccators before use. Analytical grade reagents were used. These included concentrated tetraoxosulphate (vi) acid, ethanol and Zinc dust. The concentration of acid (H₂SO₄) used for the study was 0.1M while the concentrations of the inhibitor (*Bryophyllum pinnatum*) were 0.1, 0.2, 0.3, 0.4 and 0.5 g (per liter of the acid solution).

2.2. Preparation of samples

Bryophyllum pinnatum leaves were obtained from the Botanical garden of Department of plant Biology, Bayero University Kano, Kano State, Nigeria. The plant was identified with the Herbarium Accession Number BUKHAN 0014. The leaves were washed with water; shade dried, grinded and soaked in a solution of ethanol for 48 hours. After 48 hours, the sample was filtered. The filtrate was further subjected to evaporation at 338K (65°C) in order to ensure the sample was free of ethanol. The plant extract obtained was used in preparing different concentrations of the extract by dissolving 0.1, 0.2, 0.3, 0.4 and 0.5 g of the extract in 250ml of 0.1M H₂SO₄ for the gravimetric analysis.

Corrosion monitoring Weight loss method: A previously weighed metal (zinc sheet) was completely immersed in 250 ml of the test solution (different concentrations of acid, inhibitors: as described in the section above) in an open beaker. The beaker was inserted into a water bath maintained at a temperature of 303 K. Similar experiments were repeated at 313, 323 and 333 K. In each case, the weight of the sample before immersion was measured using Scaltec high precision balance (Model

SPB31). After every 24 hours, each sample was removed from the test solution, washed in 5 % chromic acid solution (containing 1% silver nitrate) and rinsed in de ionised water.

The difference in weight for a period of 168 hours was taken as total weight loss. The inhibition efficiency (% I) for each inhibitor was calculated using the formula [8],

$$\%I = \left(1 - \frac{W_1}{W_2}\right) \times 100 \quad (1)$$

Where W_1 and W_2 are the weight losses (g/dm³) for zinc in the presence and absence of inhibitor in H₂SO₄ solution respectively. The degree of surface coverage θ is given by the equation 2;

$$\theta = \left(1 - \frac{W_1}{W_2}\right) \quad (2)$$

The corrosion rates for zinc corrosion in different concentrations of the acid and other media have been determined for 168h immersion period from weight loss using equation 3.3 below;

$$\text{Corrosionrate}(mpy) = \frac{534W}{DAT} \quad (3)$$

Where, W = weight loss (mg); D = density of specimen (g/cm³), A = area of specimen (square inches) and T = period of immersion (hour).

Potentiodynamic polarisation: The potentiodynamic current-potential curves were recorded by changing the electrode potential (Ecorr automatically with a scan rate 0.33 mV s⁻¹ from a low potential of -800 to -300 mV (SCE). Before each run, the working electrode was immersed in the test solution for 30 min to reach steady state. The corrosion rate of the structure shall be calculated through corrosion current density i_{corr} . The linear Tafel segments of the anodic and cathodic curves obtained were extrapolated to corrosion potential to obtain the corrosion current densities (i_{corr}). The inhibition efficiency (1 %) was evaluated from the measured i_{corr} values using equation 5 below;

$$\%I = \frac{i_{Corr}^0 - i_{Corr}}{i_{Corr}^0} \times \frac{100}{1} \quad (4)$$

Where i_{Corr}^0 and i_{Corr} are the uninhibited and inhibited corrosion current densities, respectively.

2.3. Chemical analysis

Phytochemical analysis of ethanol extracts of *Bryophyllum pinnatum* leaves (EEBPL) was carried out according to the method reported by Eddy [9]. For the identification of saponin, frothing and Na₂CO₃ tests were adopted. For the identification of tannin, bromine water and ferric chloride tests were used. For the identification of cardiac glycosides, Leberman's and Salkowski's tests were adopted and for the identification of alkaloid, dragendorff, Hagger and Meyer reagents were used.

2.4. FTIR Analysis

FTIR ((Fourier Transform Infra-red) analysis of EEBPL and those of the corrosion products (in the presence of the inhibitor) were carried out using Cary-630 Agilent Fourier transform infra-red spectrophotometer. The analysis was carried out by scanning the sample through a wave number range of 650cm⁻¹ to 4000cm⁻¹.

2.5. Scanning Electron Microscopy Studies

A scanning electron microscope (SEM) model JSM-5600 LV, was used to analyze the morphology of the zinc surface without and with inhibitor added. The sample was mounted on a metal stub and sputtered with gold in order to make the sample conductive, and the images were taken at an accelerating voltage of 10 kV using different magnifications.

3. Results and Discussions

3.1. Weight Loss Method (Gravimetry)

Figures 1 to 4 shows plots for the variation of weight loss with time during the corrosion of zinc in 0.1 M H₂SO₄ containing various concentrations of EEBPL at 303 to 333 K respectively. The plots generally reveal that; weight loss of zinc increases with time, but decreases with increase in the concentration of EEBPL, indicating that the corrosion rate of zinc increases with increase in the period of contact of the metal with the acid. The results also reveal that EEBPL retarded the corrosion of zinc in solution of 0.1 M H₂SO₄ hence a good adsorption inhibitor, since the corrosion rate decreases with increase in concentration. Comparing Figs. 4.1, 4.2, 4.3 and 4.4, it is evident that the weight loss of zinc increases with increase in temperature indicating that the corrosion rate of zinc also increases with increase in temperature.

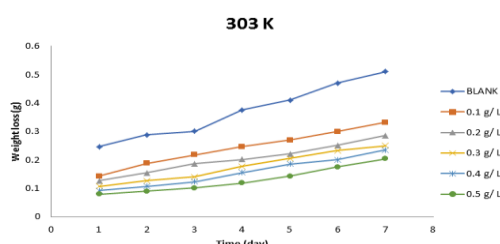


Figure 1. Variation of weight loss with time for the corrosion of zinc in 0.1 M H₂SO₄ containing various concentrations of EEBPL as inhibitor at 303 K.

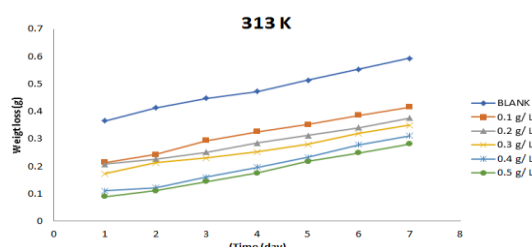


Figure 2. Variation of weight loss with time for the corrosion of zinc in 0.1 M H₂SO₄ containing various concentrations of EEBPL as inhibitor at 313 K.

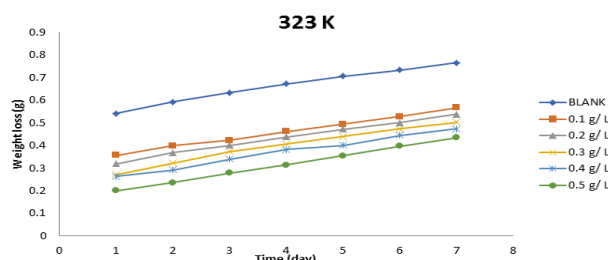


Figure 3.

Variation of weight loss with time for the corrosion of zinc in 0.1 M H_2SO_4 containing various concentrations of EEBPL as inhibitor at 323 K.

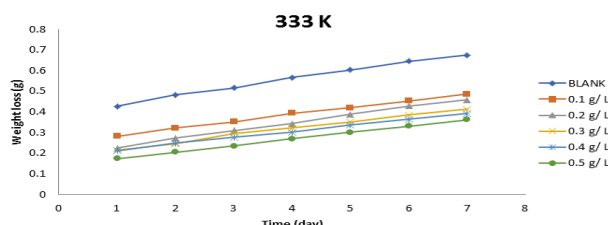


Figure 4.

Variation of weight loss with time for the corrosion of zinc in 0.1 M H_2SO_4 containing various concentrations of EEBPL as inhibitor at 333 K.

Table 1 presents values of corrosion rates of zinc at various temperatures in the absence and presence of various concentrations of EEBPL. The results indicated that in the presence EEBPL, the corrosion rate is decreased, even as the concentration of the extract increases. The trend for the decrease is presented graphically in Fig. 5. The plots generally reveal that the decrease in corrosion rate varies with the concentration of EEBPL. Values of inhibition efficiency of EEBPL calculated from equation 1 are also presented in Table 2. From the results obtained, the inhibition efficiency is seems to increase with concentration of EEBPL. This may be attributed to the decrease in the protective nature of the inhibitive film formed on the metal surface (or desorption of the inhibitor molecules from the metal surface) at higher temperatures. This suggests that the mechanism of inhibition of *Bryophyllum pinnatum* leaves extract for the corrosion of zinc in solution of 0.1M H_2SO_4 is physical adsorption. According to Ameh [10], a physical adsorption mechanism is characterised with a decrease in inhibition efficiency with temperature as opposed to chemical adsorption mechanism, where inhibition efficiency is expected to increase with increase in temperature. The inhibitive action of the *Bryophyllum pinnatum* leaves extract is due mainly to the presence of saponins, terpenes, flavanoids, phlobatanins, anthraquinones, cardiac glycosides and alkaloids present in the plant extracts. These compounds contain heteroatoms such as oxygen, nitrogen or aromatic rings with π bonds in their molecules, which serve as centres for adsorption onto the metal surface.

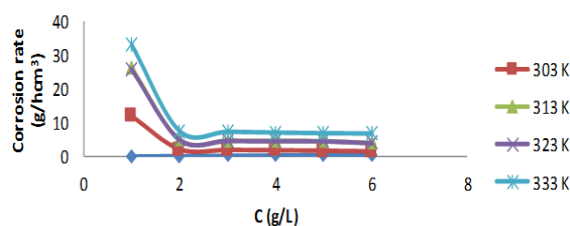


Figure 5.

Variation of corrosion rate of zinc with concentration of EEBPL at various temperatures.

Table 1.

Corrosion rate of zinc in the presence and absence of various concentrations of EEBPL.

C (g/L)	Corrosion rate ($gcm^{-2}h^{-1}$)			
	303 K	313 K	323 K	333 K
Blank	0.0001201	0.0002625	0.0002581	0.0003336
0.1	0.000019	0.0000493	0.0000484	0.000075
0.2	0.0000172	0.0000463	0.0000452	0.000073
0.3	0.0000162	0.0000451	0.0000443	0.0000705
0.4	0.0000149	0.0000452	0.000044	0.0000685
0.5	0.0000131	0.0000394	0.0000384	0.0000672

Table 2.

Degree of surface coverage and Inhibition efficiency of various concentrations of EEBPL for Zinc.

C (g/L)	Degree of surface coverage (θ)				Inhibition efficiency (%)			
	303 K	313 K	323 K	333 K	303 K	313 K	323 K	333 K
0.1	0.839	0.811	0.811	0.775	83.91	81.09	81.08	77.45
0.2	0.854	0.824	0.823	0.781	85.4	82.36	82.34	78.08
0.3	0.864	0.827	0.827	0.788	86.39	82.71	82.68	78.8
0.4	0.876	0.828	0.828	0.794	87.62	82.83	82.79	79.4
0.5	0.891	0.85	0.849	0.797	89.11	85	84.9	79.66

Also, in Table 2 for the values of degree of surface coverage, the results show similar trend to those of inhibition efficiencies, this is because the degree of surface coverage is directly proportional to the inhibition efficiency. It can be seen that the degree of surface coverage increases as the concentration of the inhibitor increases. This is as result of the EEBPL forming compact layer on the zinc metal, preventing further corrosion of the zinc. However, as the temperature increases, the degree of surface coverage decreases. This is due to the fact that desorption of the inhibitor from the surface of the zinc metal took place under this condition.

3.2. Electrochemical Measurement

The results obtained from the potentiodynamic polarization (PDP) (anodic and cathodic) study for the corrosion of zinc in 0.1 M H₂SO₄ solution in the presence and absence of the various concentration of the inhibitor are presented in Figure 6. The electrochemical parameters derived from these plots are presented in Table 3. From the results presented, it can be seen that both the corrosion potential (E_{corr}) and corrosion current densities (i_{corr}) decrease on addition of the inhibitor (EEBPL) to 0.1 M H₂SO₄. When the inhibitor concentration was increased progressively from 0.1 g/L to 0.5 g/L, values of corrosion potential (E_{corr}) were shifted more negatively. This is an indication of a mixed-type corrosion inhibition mechanism [11]. The calculated IE% obtained follows similar trend as that in weight loss measurement, indicating that the plant extracts inhibited the corrosion of the zinc metal.

Table 3.

Potentiodynamic polarization resistant data for the corrosion of zinc in 0.1 M H₂SO₄ containing various concentrations of EEBPL at 303K.

Conc.(g/l)	I_{corr} (μ A)	E_{corr} (mV)	IE %
Blank	1179.022	-864.951	-
0.1	516.461	-869.382	56.2
0.2	343.09	-934.371	70.91
0.3	286.531	-952.042	75.7
0.4	187.682	-1109.52	84.09
0.5	128.562	-1223.41	89.1

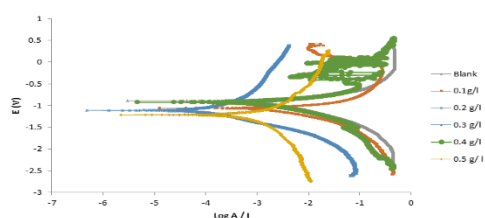


Figure 6.

Polarization curve for the corrosion of zinc in 0.1 M H₂SO₄ in the presence and absence of various concentration of EEBPL at 303K.

In Table 3, the values of corrosion current density (I_{corr}) also decreased in the presence of increased concentration of EEBPL which suggests that the rate of electrochemical reaction was reduced due to the formation of a barrier layer over the zinc metal surface by the inhibitor [11]. The inhibition efficiency results of the inhibitor were calculated from the corrosion current values according to equation 5, and the values are presented in Table 3. From the values, it can be seen that the inhibition efficiency showed a steady increase following increased inhibitor concentration from 0.1 g/L to 0.5 g/L. This increase in inhibition efficiency (from 0 to 89.10 %) as compared to the blank value indicates a reduction in zinc metal corrosion rate through the formation of adsorbed protective film against corrosion attack at the metal/electrolyte interface [10].

3.3. Effect of Temperature

Temperature affects the rate of any chemical reaction including corrosion reaction. The effect of temperature on the rate of corrosion of zinc can be modelled using the Arrhenius equation, which can be expressed as follows;

$$CR = A \exp\left(\frac{-E_a}{RT}\right) \quad (5)$$

Where CR is the corrosion rate of zinc in solution of H₂SO₄, A is the Arrhenius constant or pre-exponential factor, E_a is the minimum energy needed for the corrosion reaction to start (i.e activation energy), R is the universal gas constant and T is the absolute temperature. Logarithm of both sides of equation 6 yields equation 7 as expressed below,

$$\log(CR) = \ln(A) - \frac{E_a}{RT} \quad (6)$$

The implication of equation 7 is that a plot of $\log(CR)$ versus $1/T$ should be linear with slope equals to $-E_a/R$ and intercept equals to $\ln(A)$. Fig. 7 shows the Arrhenius plots for the corrosion of zinc in the absence and presence of various concentrations of EEBPL. Values of Arrhenius parameters calculated from the plots are presented in Table 4. From the results obtained, it is evident that excellent degree of linearity (R^2 ranged from 0.9922 to 0.9999) were obtained in all cases indicating the application of the Arrhenius model to the inhibited and uninhibited corrosion reaction of zinc.

Table 4.

Arrhenius parameters for the inhibition of the corrosion of zinc by various concentrations of EEBPL.

C (g/L)	Slope	$\ln(A)$	E_a (J/mol)	R^2
0.1 M H ₂ SO ₄	3.4645	13.94	27.71	0.9922
0.1g/L of (BP)	4.552	15.68	36.73	0.9997
0.2g/L of (BP)	4.7305	16.24	38.29	0.9999
0.3g/L of (BP)	4.892	16.65	40.54	0.9996
0.4g/L of (BP)	5.1491	17.41	41.6	0.9975
0.5g/L of (BP)	5.4747	18.33	44.41	0.9999

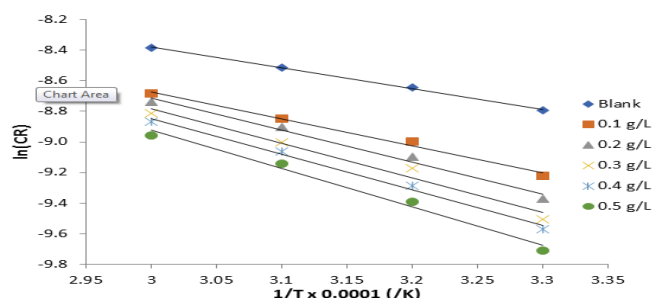


Figure 7.

Arrhenius plot for the corrosion of zinc in the presence of *Bryophyllum pinnatum* leaves extract as an inhibitor at various temperatures.

Value of the activation energy for the blank was 27.70 J/mol. In the presence of 0.1, 0.2, 0.3, 0.4 and 0.5 g /L of the inhibitor (EEBPL), values of E_a were found to be; 36.73, 38.29, 40.54, 41.60 and 44.41 kJmol⁻¹ respectively. The inhibitor (EEBPL), thus increases the corrosion activation energies for zinc in 0.1 M H₂SO₄ thereby slowing the corrosion process. Therefore, the corrosion of zinc is retarded by the presence of EEBPL, and the ease of adsorption of the inhibitor on the surface of the metal increases with increasing concentration. According to Ameh 2015, values of activation energy less than 80 kJ/mol is associated with the mechanism of physical adsorption while those more than 80 kJ/mol points toward the mechanism of chemical adsorption. Hence the mechanism of adsorption of EEBPL on the surface of zinc is consistent with charge transfer from charged inhibitor to charged metal surface, which favours physical adsorption [12].

3.4. Thermodynamics Considerations

Thermodynamic parameters (including enthalpy and entropy of adsorption) for the adsorption of EEBPL on the surface of zinc was investigated using Eyring transition state equation, which can be expressed as follows [12];

$$\ln\left(\frac{CR}{T}\right) = \ln\left(\frac{R}{Nh}\right) + \frac{\Delta S_{ads}^0}{R} - \frac{\Delta H_{ads}^0}{RT} \quad (7)$$

From equation 4.3, a plot of $\ln(CR/T)$ versus $1/T$ should be linear with slope and intercept equal to $\frac{\Delta H_{ads}^0}{R}$ and $\ln\left(\frac{R}{Nh}\right) + \frac{\Delta S_{ads}^0}{R}$ respectively. Fig. 8 shows the transition state plot for the corrosion of zinc in 0.1 M H₂SO₄ containing various concentrations of EEBPL. Thermodynamic parameters deduced from the plots are presented in Table 5. From the results obtained, R² values are very close to unity indicating the application of the Transition state model to the studied corrosion reaction. Values of standard enthalpy change deduced from the plots were found to be negative and ranged from -35.22 to -42.90 J/mol. These values are greater than that of the blank (enthalpy change for the blank = -26.18 J/mol) and tend to increase with increase in concentration of EEBPL. Therefore, the corrosion of zinc in H₂SO₄ solution is strongly retarded by EEBPL and that the ease of adsorption of the inhibitor on the metal surface increases with increasing concentration. On the other hand, the entropy of activation is positive both in the absence and presence of inhibitor (EEBPL). This is an indication that for the adsorption of EEBPL to be spontaneous, the enthalpy values should be negative as found in the present study. The increase in entropy implies disordering that took place in going from reactants to the activated complex. The negative sign of enthalpy of adsorption indicated the exothermic nature of zinc metal dissolution process.

Table 5. Transition state parameters for the inhibition of the corrosion of zinc by various concentrations of EEBPL.

C	Slope	Intercept	ΔS_{ads}^0 (J/mol)	ΔH_{ads}^0 (J/mol)	R ²
Blank	3.1493	7.1829	257.26	-26.18	0.9908
0.1	4.2368	8.9294	271.78	-35.22	0.9997
0.2	4.4353	9.487	276.42	-36.88	1
0.3	4.578	9.8938	279.8	-38.06	1
0.4	4.8339	10.652	286.1	-40.19	0.9972
0.5	5.1595	11.58	293.82	-42.9	0.9999

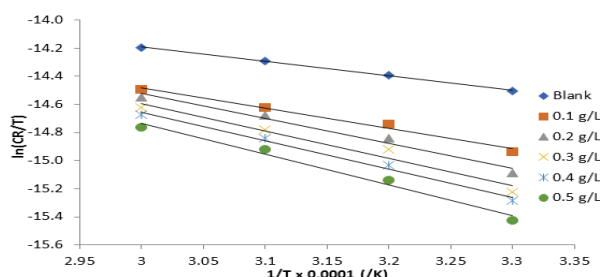


Figure 8.

Transition state plot for the inhibition of the corrosion of zinc in 0.1 M H₂SO₄ by various concentrations of EEBPL.

4.5. Adsorption Considerations

The adsorption characteristics of EEBPL for zinc was investigated using adsorption isotherms including Langmuir, Freundlich, Flory-Huggins, El awardy *et al.*, Bockris-Swinkels and Temkin isotherms. Fitness of the data obtained for the degree of surface coverage reveals that Langmuir model best described the adsorption of EEBPL on the surface of zinc

The Langmuir adsorption model can be expressed as follows [13].

$$\log\left(\frac{C}{\theta}\right) = \log b_{ads} - \log C \quad (8)$$

Where C is the concentration of EEBPL in the bulk electrolyte, θ is the degree of surface coverage of the inhibitor and b_{ads} is the equilibrium constant of adsorption, which is related to the standard free energy of adsorption according to equation 10

$$b_{ads} = -\frac{1}{55.5} \exp\left(\frac{\Delta G_{ads}^0}{RT}\right) \quad (9)$$

Figure 9 shows the Langmuir plots developed through equation 4.4, while adsorption parameters (including values of ΔG_{ads}^0 , calculated from equation 10) deduced from the Langmuir plots are presented in Table 6. The constant value of 55.5 is the concentration of water in solution in mol/l; since ΔG_{ads} are below 40 kJ/mol (ΔG_{ads} threshold value), it corroborates that the adsorption process is physisorption [14]. The negative values of ΔG_{ads} indicated spontaneous adsorption of the inhibitor on the zinc metal surface. Slope values are seen to proximate unity, which suggest that there is little or no interaction between the inhibitor and the metal. Excellent correlations obtained for the different temperatures studied confirm the application of Langmuir isotherm to the adsorption of EEBPL on zinc. Calculated values of the free energy are within the range of values expected for the mechanism of physical adsorption, hence the adsorption of EEBPL on the surface of zinc is consistent with the mechanism of physical adsorption [15].

Table 6. Langmuir parameters for the adsorption of EEBPL.

T (K)	Slope	$\log b_{ads}$	ΔG_{ads}^0 (kJ/mol)	R ²
303	0.9646	0.0425	-10.36	0.9999
313	0.9762	0.0681	-10.51	0.9998
323	0.9767	0.0686	-10.52	0.9999
333	0.9819	0.0936	-10.66	1

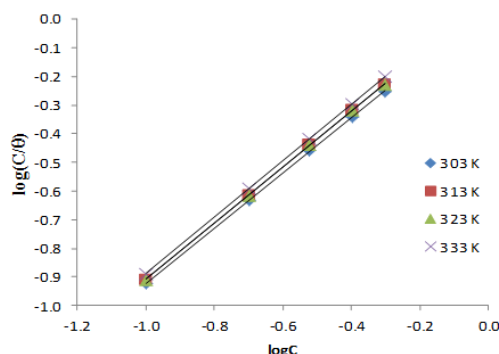


Figure 9.
Langmuir isotherm for the adsorption of EEBPL on the surface of zinc.

3.6. Photochemical Constituents of the Inhibitor (EEBPL)

Table 7 presents the phytochemical constituents of EEBPL. From the results, it is significant to note that the extract studied contain saponin, terpenes, tannins, flavanoid, phlobatanins, anthraquinones, cardiac glycoside and alkaloids. From, the point of view of corrosion inhibition, these phytochemicals are expected to be good corrosion inhibitors, since they contain long chain of carbon-carbon single and double bonds having π bonds that contain π electrons for bond formation with the zinc metal, thereby preventing corrosion of the zinc metal. Umoren, et al. [16] have reported that saponins, tannins and alkaloids are active constituents of most green inhibitors. Hence, the inhibition efficiency of the *Bryophyllum pinnatum* leaves extract observed may be due to the presence of some or all of the mentioned phytochemicals. This is because they are organic compounds that are characterized by the presence of heteroatoms [5]. Therefore, the inhibition of the corrosion of zinc by EEBPL is due to the formation of chelates between zinc and some phytochemicals constituents of the extract.

Table 7.
Phytochemical constituents of EEBPL.

Phytochemicals	<i>Bryophyllum pinnatum</i> (BP)
Saponins	+++
Terpenes	+++
Tannins	+
Flavonoid	++
Phlobatannins	+++
Anthraquinones	+++
Cardiac glycoside	+++
Alkaloids	+++

Note: ** +++ = Highly present, ++ = Moderately present, - = Absent or presence in negligible quantity.

3.7. FTIR Study

In this study, ethanol extract of *Bryophyllum pinnatum* leaves (EEBPL) has been found to be a good corrosion inhibitor for zinc metal. The inhibition potential of the extract can be explained in terms of interaction between the metal and the inhibitor. Most efficient corrosion inhibitors are long-carbon chain or aromatic compounds that have heteroatoms such as; N, S, P, and O in their system. The presence of π -electron rich functional groups has also been found to enhance inhibition efficiency of a corrosion inhibitor [10].

Fig. 10 shows IR spectrum of EEBPL while Fig. 11 shows the IR spectrum of the corrosion product of zinc when 0.5 g/L of EEBPL was used as an inhibitor.

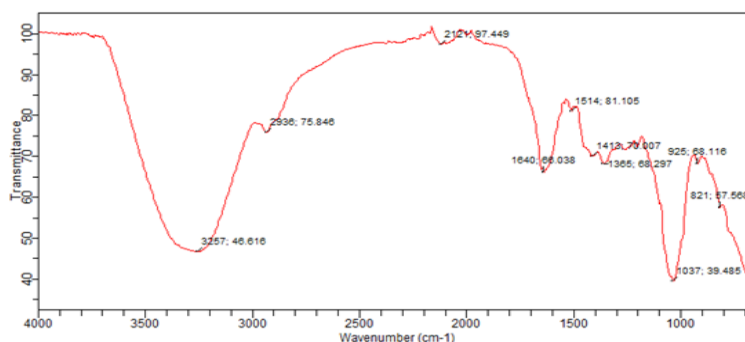


Figure 10.
FTIR spectrum of EEBPL (*Bryophyllum pinnatum* leaves extract).

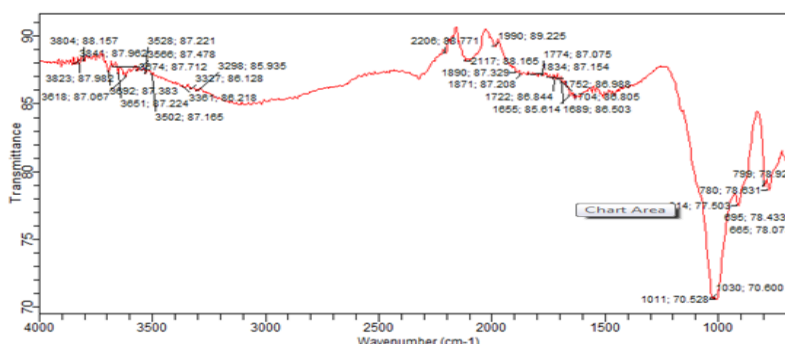


Figure 11.
FTIR spectrum of the corrosion product of zinc when 0.5 g/L of EEBPL was used as an inhibitor.

Table 8 presents frequencies and functional group assignments that are associated with the absorption of IR by EEBPL, while Table 9 presents frequencies and functional group assignments that are associated with the absorption of IR by the corrosion product. From the IR spectrum of EEBPL, OH stretch at 3257 cm^{-1} , CN stretch at 1365 cm^{-1} , NH bend at 1514 cm^{-1} , CH stretch at 2936 cm^{-1} , C=C stretch at 1640 cm^{-1} , C≡C stretch at 2121 cm^{-1} , CH rock at 1365 cm^{-1} , C-O stretch at 1037 cm^{-1} , CH bend at 821 and at 925 cm^{-1} were identified. The corrosion product of the studied metal in the presence of inhibitor revealed that CH bend at 821 and 925 cm^{-1} were shifted to 799 and 914 cm^{-1} , the C-O stretch at 1037 cm^{-1} were shifted to 1030 cm^{-1} , the C=C Stretch at 1640 cm^{-1} was shifted to 1655 cm^{-1} , C≡C stretch at 2121 cm^{-1} was shifted to 2117 cm^{-1} , the OH stretch at 3257 cm^{-1} was shifted to 3298 cm^{-1} . The shifts in the frequencies of vibration indicate that there is interaction between the inhibitor and the metal surface. Also, the N-H bend scissoring at 1514 cm^{-1} was absent in the spectrum of the corrosion product of zinc suggesting that this functional groups were used in the adsorption of the inhibitor to the metal surface. On the other hand the C-H bend at 665 cm^{-1} , C=O stretch at 1834 cm^{-1} , the C-H stretch at 1990 cm^{-1} , the C-N stretch at 2206 cm^{-1} , the OH stretch free hydroxyl at 3618 cm^{-1} and the NH stretch at 3361 cm^{-1} were new to the spectrum of the corrosion product indicating that new bonds were formed.

Table 8.

Wave number and Intensity of FTIR of EEBPL (*Bryophyllum pinnatum* leaves extract).

Wave no (cm^{-1})	Intensity	Assigned functional group
821	57.568	C-H bend, phenyl ring substitution band
925	58.116	C-H bend, alkene
1037	39.485	C-O stretch, carboxylic acid, ether, ester, alcohol
1365	68.297	C-N stretch, amine
1413	70.007	C-H scissoring and bending, alkanes
1514	81.105	N-H bend, amines
1640	66.038	C=C stretch, alkene
2121	97.449	C≡C stretch, alkyne
2936	75.846	C-H stretch
3257	46.616	O-H stretch, alcohol, phenol

3.8. Scanning Electron Microscopy (SEM)

The SEM analysis was carried out using different magnifications of $150\times$, $500\times$ and $1500\times$, and the results are presented as follows;

Fig. 12 (A), shows the scanning electron micrograph of pure zinc metal, while Fig. 12 (B) and (C), show the scanning electron micrograph of zinc metal in the absence and presence of EEBPL respectively. For the zinc metal (B) in H_2SO_4 , a great degree of corrosion was observed when compared to the pure zinc metal in (A). This can be evidently seen as the surface was rough and coarse, due to the distortion of the surface layer by the corrodent (acid). The degree of corrosion however reduced drastically in zinc metal (C) which was in contact with the acid solution in the presence of EEBPL as inhibitor. This shows that the leave extract inhibited the corrosion of zinc in H_2SO_4 . This was as a result of the leaves extract forming multiple films on the zinc surface for adsorption. Therefore, EEBPL prevented the corrosion of zinc by forming a protective layer on its surface.

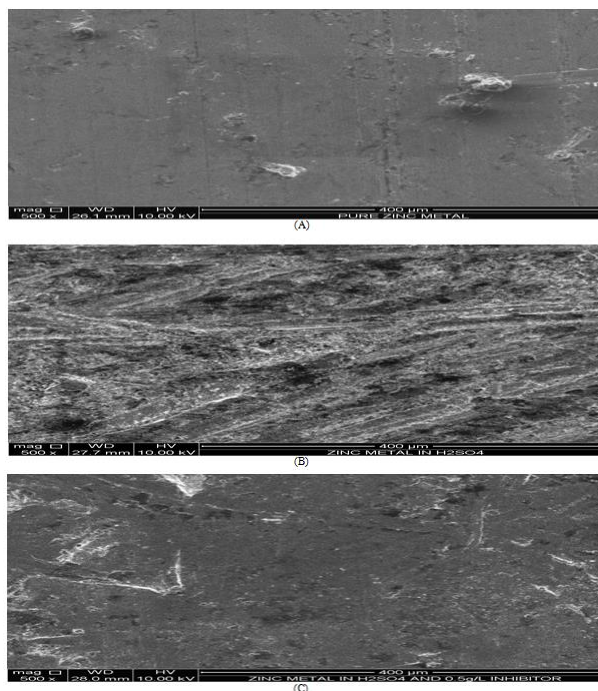


Figure 12.

Scanning electron micrographs of (A) Pure Zinc metal, (B) Zinc metal in Corrodent($0.1\text{M H}_2\text{SO}_4$), (C) Zinc Metal in Corrodent in the presence of EEBPL (As an inhibitor) at magnification of $1500\times$.

4. Conclusion

Corrosion inhibition of zinc metal by ethanol extract of *Bryophyllum pinnatum* leaves (EEBPL) is as a result of the phytochemical constituents of the plant extract. These phytochemicals facilitated the adsorption behaviour of the inhibitor onto the metal (zinc) surface. The adsorption of EEBPL on the surface of zinc is best described by the Langmuir adsorption model. All values of the standard Gibbs energy of adsorption are negative (spontaneous adsorption process) and lower in absolute values than 40 kJ mol^{-1} . Also, the activation energies, E_a , of the inhibited systems increased considerably as the concentration of the inhibitor increased progressively. These results confirm that physisorption mechanism controls the adsorption phenomenon. The corrosion product of zinc metal in the presence of EEBPL is IR active, whereas the corrosion product of zinc metal is not IR active. The IR spectrum of the corrosion product of zinc metal in the presence of EEBPL confirmed that the extract actually inhibited the corrosion of zinc by being adsorbed onto the surface of the zinc metal and indicating interaction

between the inhibitor and the surface. Inhibition efficiency of the inhibitor correspondingly increased with an increase in the concentration of EEBPL in 0.1M H₂SO₄. The results of the analysis revealed that both the inhibition efficiency and degree of surface coverage decreases as temperature increases. The negative values of ΔG_{ads} show that adsorption of inhibitor on surface of the zinc metal is spontaneous.

Conclusively, the ethanol extract of *Bryophyllum pinnatum* leaves (EEBPL) is a good, economical, biodegradable and eco-friendly adsorption inhibitor for the corrosion of zinc metal in 0.1M H₂SO₄.

Table 9.

Wave number and Intensities of FTIR of corrosion product of *Bryophyllum pinnatum* extract as inhibitor of zinc in 0.1M H₂SO₄.

Wave No (cm-1)	Intensity	Assigned functional group
665	78.073	C-H bend, alkynes
695	78.433	C-H bend, alkynes
780	78.631	C-H bend, phenyl ring substitution band
799	78.928	C-H bend, phenyl ring substitution band
914	77.503	C-H bend, alkene
1011	70.528	C-O stretch, carboxylic acid, ether, ester, alcohol
1030	70.6	C-O stretch, carboxylic acid, ether, ester, alcohol
1655	85.614	C=C stretch, alkenes
1689	86.503	C=C stretch, aromatic ring
1704	86.805	C=C stretch, aromatic ring
1722	86.844	C=C stretch, aromatic ring
1752	86.968	C=C stretch, aromatic ring
1774	87.075	C=C stretch, aromatic ring
1834	87.154	C=O stretch
1871	87.208	C=O stretch
1890	87.329	C=O stretch
1990	89.225	C-H stretch, phenyl ring subst.
2117	88.165	C≡C stretch, alkyne
2206	88.771	C-N stretch, amine
3298	85.935	O-H stretch, alcohol, phenol
3327	86.128	N-H stretch, amine
3361	86.218	C-H stretch
3502	87.165	C-H stretch
3528	87.221	C-H stretch
3566	87.478	C-H stretch
3618	87.067	O-H stretch, free hydroxyl
3651	87.224	O-H stretch, free hydroxyl
3674	87.712	O-H stretch, free hydroxyl
3692	87.383	O-H stretch, free hydroxyl
3804	88.157	C-H stretch
3823	87.982	C-H stretch
3841	87.962	C-H stretch

References

- [1] O. Abiola, N. Oforka, E. Ebenso, and N. Nwinuka, "Eco-friendly corrosion inhibitors: The inhibitive action of Delonix Regia extract for the corrosion of aluminium in acidic media," *Anti-Corrosion Methods and Materials*, vol. 54, no. 4, pp. 219-224, 2007. <https://doi.org/10.1108/00035590710762357>
- [2] A. El-Etre, "Inhibition of aluminum corrosion using opuntia extract," *Corrosion Science*, vol. 45, no. 11, pp. 2485-2495, 2003. [https://doi.org/10.1016/S0010-938X\(03\)00066-0](https://doi.org/10.1016/S0010-938X(03)00066-0)
- [3] M. Bouklah and B. Hammouti, "Thermodynamic characterisation of steel corrosion for the corrosion inhibition of steel in sulphuric acid solutions by Artemisia," *Portugaliae Electrochimica Acta*, vol. 24, no. 4, pp. 24457-24468, 2006. <https://doi.org/10.4152/pea.200604457>
- [4] E. Oguzie, "Inhibition of acid corrosion of mild steel by Telfaria occidentalis extract," *Pigment & Resin Technology*, vol. 34, no. 6, pp. 321-326, 2005. <https://doi.org/10.1108/03699420510630336>
- [5] N. Eddy and P. Mamza, "Inhibitive and adsorption properties of ethanol extract of seeds and leaves of Azadirachta indica on the corrosion of mild steel in H₂SO₄," *Portugaliae Electrochimica Acta*, vol. 27, no. 4, pp. 443-456, 2009. <https://doi.org/10.4152/pea.200904443>
- [6] M. Nwankwo, P. Nwobasi, S. Neife, and N. Idenyi, "Statistical studies of the inhibition characteristics of acidified ocimum basilicum on engineering mild steel," *Journal of Metallurgical Engineering*, vol. 2, pp. 155-160, 2013. <https://doi.org/10.4236/jmmce.2013.160057>
- [7] A. A. Hadi, "Use reed leaves as a natural inhibitor to reduce the corrosion of low carbon steel," *International Journal of Engineering Research and General Science*, vol. 3, no. 3, pp. 514-521, 2015.
- [8] N. A. Negm, M. A. Yousef, and S. M. Tawfik, "Impact of synthesized and natural compounds in corrosion inhibition of carbon steel and aluminium in acidic media," *Recent Patents on Corrosion Science*, vol. 3, no. 1, pp. 58-68, 2013. <https://doi.org/10.2174/2210683911303010007>
- [9] N. Eddy, "Ethanol extract of phyllanthus amarus as a green inhibitor for the corrosion of mild steel in H₂SO₄," *Portugaliae Electrochimica Acta*, vol. 27, no. 5, pp. 579-589, 2009. <https://doi.org/10.4152/pea.200905579>
- [10] P. O. Ameh, "A comparative study of the inhibitory effect of gum exudates from khaya senegalensis and albizia ferruginea on the corrosion of mild steel in hydrochloric acid medium," *International Journal of Metals* p. 824873, 2015. <https://doi.org/10.1155/2015/824873>
- [11] P. Ameh and P. Ukoha, "Eddy no experimental and quantum chemical studies on the corrosion inhibition potential of phthalic acid for mild steel in 0.1 M H₂SO₄," *Chemical Science Journal*, vol. 6, pp. 1- 8, 2015.
- [12] N. Eddy, "Theoretical study on some amino acids and their potential activity as corrosion inhibitors for zinc in HCl," *Molecular Simulation*, vol. 35, pp. 354-363, 2010. <https://doi.org/10.1080/08927020903483270>
- [13] E. Ogoko, S. Odoemelam, B. Ita, and N. Eddy, "Adsorption and inhibitive properties of clarithromycin for the corrosion of Zn in 0.01 to 0.05 M H₂SO₄," *Portugaliae Electrochimica Acta*, vol. 27, no. 6, pp. 713-724, 2009. <https://doi.org/10.4152/pea.200906713>
- [14] E. Ebenso, U. Ekpe, U. Ibok, S. Umoren, and E. Jackson, "Trans," *SAEST*, vol. 39, pp. 117-123, 2004.
- [15] N. O. Eddy, "Experimental and theoretical studies on some amino acids and their potential activity as inhibitors for the corrosion of mild steel, part 2," *Journal of Advanced Research*, vol. 2, no. 1, pp. 35-47, 2011. <https://doi.org/10.1016/j.jare.2010.08.005>
- [16] S. Umoren, I. Obot, L. Akpabio, and S. Etuk, "Adsorption and corrosive inhibitive properties of Vigna unguiculata in alkaline and acidic media," *Pigment & Resin Technology*, vol. 37, no. 2, pp. 98-105, 2008. <https://doi.org/10.1108/03699420810860455>